

Received August 30, 2019, accepted September 29, 2019, date of publication October 23, 2019, date of current version November 20, 2019.

Digital Object Identifier 10.1109/ACCESS.2019.2949223

# Imaging Performance of a Diffractive Corneal Inlay for Presbyopia in a Model Eye

DIEGO MONTAGUD-MARTÍNEZ<sup>1</sup>, VICENTE FERRANDO<sup>1</sup>, FEDERICO MACHADO<sup>1</sup>,  
JUAN A. MONSURIU<sup>1</sup>, AND WALTER D. FURLAN<sup>2</sup>

<sup>1</sup>Centro de Tecnologías Físicas, Universitat Politècnica de València, 46022 Valencia, Spain

<sup>2</sup>Departamento de Óptica y Optometría y Ciencias de la Visión, Universitat de València, 46100 Burjassot, Spain

Corresponding author: Walter D. Furlan (walter.furlan@uv.es)

This work was supported in part by the Ministerio de Economía y Competitividad under Grant DPI2015-71256-R, and in part by the Generalitat Valenciana, Spain, under Grant PROMETEO/2019/048. The work of D. Montagud-Martínez and V. Ferrando was supported by the Universitat Politècnica de València, Spain, under Grant FPI-2016 and Grant PAID-10-18.

**ABSTRACT** In this work we evaluated the imaging properties of the Diffractive Corneal Inlay (DCI), a novel type of corneal implant working by diffraction that we proposed for the treatment of presbyopia. ZEMAX OpticStudio software was employed for the numerical assessment, with simulations performed in a human-based eye model. In the ray tracing analysis, we used the Modulation Transfer Function (MTF), the Area under the MTF (AMTF), and the Point Spread Function (PSF). The theoretical performance of the DCI under different situations was evaluated in comparison with a commercially available pinhole based corneal inlay. Finally, real images were obtained experimentally in vitro in a model eye with inlays prototypes. The obtained results allow to state that the DCI exhibits a very high light throughput, improved imaging capabilities for far and near objects, and robustness against decentrations.

**INDEX TERMS** Corneal inlays, diffractive lenses, Presbyopia, optical design.

## I. INTRODUCTION

Modelling the imaging process in the human eye is far from being considered as “conventional” by an optical engineer because of the complex environment in which this process takes place. Opposite to many artificial optical systems, in which lenses are centered on the optical axis and separated by air, in the eye, the ocular surfaces are not perfectly aligned and several tissues and fluids with different refractive indexes and internal structure are present in the way of light from the outside world to the retina. In particular, a challenging problem for an optical engineer is the design of optical devices for the treatment of presbyopia because it deals with the restitution of the eye’s ability to see clearly at multiple distances, which was progressively lost with age by the decline of the amplitude of accommodation. In conjunction with multifocal intraocular lenses, corneal inlays are one of the most recent advances in this field. These devices are implanted inside the cornea with a surgical procedure that includes the creation of ‘pockets’ by precise femtosecond lasers within the corneal stroma.

The associate editor coordinating the review of this manuscript and approving it for publication was Huimin Lu .

Based on their physical principles, corneal inlays can be classified into different categories: refractive inlays, small aperture inlays, and diffractive inlays. Refractive corneal inlays act locally at central part of the cornea either, by altering locally its refractive index (Presbia Flexivue Microlens, Presbia Cooperatief) or by modifying its curvature (Raindrop Near Vision inlay, which is no longer in the market) [1], [2]. A recent review of the corneal inlays currently used for the correction of presbyopia [3], concluded that refractive inlays are very limited, most likely because they induce high order aberrations that result in a decreased contrast sensitivity.

On the other hand, Small Aperture Corneal Inlays (SACIs) with the commercial name Kamra®(Acufocus, Inc.) are often used today owing to the positive outcomes achieved in improved uncorrected near and intermediate vision [3], [4]. This device is simply an opaque disc made of a biocompatible material (polyvinylidene fluoride impregnated with carbon nanoparticles) with a central hole acting as pinhole-like aperture that produces an extended depth of focus. To facilitate the flow of nutrients to the cells of the corneal stroma, it has a reduced external diameter, and more than 8,000 micropores, in a size range of 5–11  $\mu\text{m}$  diameter. However, its reduced light throughput, forces its implantation only in one

(the non-dominant) eye creating a “modified monovision” situation [1]. This condition, added to the light diffracted by the randomly distributed micro-holes across the implant, produce some drawbacks, including: compromised distance visual acuity [5], a potential detrimental effect on the binocular summation ratio [6], a marked interocular differences in visual latency, and a Pulfrich effect. [7]. Another visual function compromised by this inlay is stereoacuity, which could suffer a deterioration with respect to natural conditions, especially for near and intermediate distances [8].

In a recent paper [9], we have demonstrated that the diffraction intrinsically originated by the pores in the SACI can be harnessed to provide a focus for near distance vision, in a similar fashion as a photon sieve [10], [11] does. In practice, we have combined the photon sieve and the SACI pinhole-effect concepts to develop a novel class of corneal implants: the diffractive corneal inlays (DCIs). In this way, we were able to turn the negative diffractive effects of SACI from a disadvantage into a significant advantage, because the micro-holes in the DCI would not just permit the flow of nutrients, but also create a diffractive focus for near vision. Moreover, we announced that by optimizing the size and spatial distribution of the holes, different designs would be able to vary the addition and the relative intensity between near and far foci. In this way, this new type of prosthesis could allow doctors to customize the treatment of presbyopia. In that previous work, the focusing properties of the DCI were investigated, like a conventional diffractive optical element, analyzing its diffraction pattern by computing the Point Spread Function (PSF) along the optical axis using the Fresnel approximation. Experimental results of the axial PSF in free space propagation were also provided with a DCI simulated in a liquid crystal SLM. These preliminary results demonstrated that the DCI had a better performance than the SACI [9]. With these promising findings, the next step is to investigate the potential benefits in image formation by DCIs by means of merit functions that evaluate the eye’s quality of vision in a more realistic environment. Therefore, the purpose of this study is to assess the image quality provided by an optimized version of the DCI, in comparison with the SACI in an accurate model eye. Zemax OpticStudio design software was employed to compare the performance of both inlays in the Liou-Brennan model eye. This model is especially suitable for this study for two main reasons: First, it reflects average biometrical data from a large group of individuals, incorporating a realistic amount of spherical aberration and a grin based model crystalline lens [12], [13]. Second, it takes into consideration the angle kappa, the angle between the line of sight and the pupillary axis, which is fundamental to explore the robustness of our proposal against decentrations for different pupil diameters. In fact, for the SACI it was demonstrated that the centration of the inlay is critical to achieve good vision [14]. Finally, in order to confirm our theoretical predictions, experimental results were also obtained with a model eye mounted in an optical bench in accordance with the ISO 11979-9 Standard.

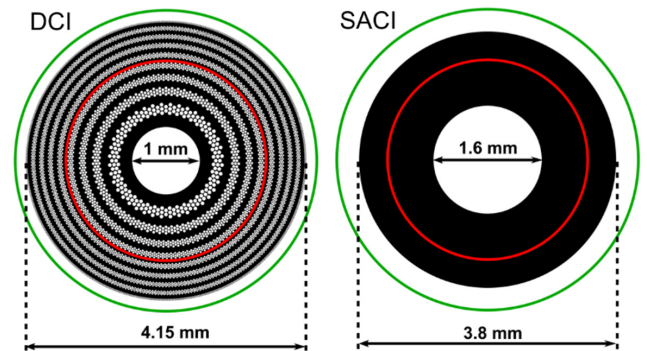


**FIGURE 1.** Diagrams of the corneal inlays evaluated in this study. The red and green circles represent 3.0 mm and 4.5 mm pupil diameters respectively.

## II. METHODS

### A. CORNEAL INLAYS

The DCI model evaluated in this study consisted in a disk of 4.15 mm diameter with a central hole of 1.00 mm diameter surrounded by 8 rings conformed by a total of 6395 holes of different size, being the smallest ones of 11  $\mu\text{m}$  diameter. It was designed to provide a near diffractive focus corresponding to a nominal addition of +2.50 D. For comparison, a completely opaque SACI with the dimensions of the Kamra® has been evaluated in parallel. Sketches of the evaluated DCI and SACI are shown in Fig. 1. The thickness of both inlays were assumed as 5  $\mu\text{m}$ .

### B. NUMERICAL METHODS

Zemax OpticStudio design software (version 18.7, LLC, Kirkland, WA, USA) was employed to simulate the effects of both inlays in the Liou-Brennan model eye. This model eye is characterized by aspheric corneal elements; a gradient index crystalline lens; a decentered iris pupil (0.50 mm in the nasal direction); and a tilted visual axis, (5 degrees relative to the optical axis) [12]. The model data is shown in Table 1. The inlays were located in the model eye at 0.25 mm from the anterior corneal surface as “User Defined Apertures” (.uda file). In the simulations, the same values for the radius of curvature and for the asphericity of the anterior corneal surface were considered for both inlays. The original version of the Liou-Brennan model eye did not have a value for the retinal curvature. However, considering that the curvature of the retina may have an impact on image quality with inlay decentration, in this work we have included the retina with a  $-12$  mm radius. Two different pupils (iris) diameters were evaluated: 3.0 mm and 4.5 mm (emulating photopic and mesopic conditions). To better appreciate the sensitivity of the inlays to decentration, we assumed monochromatic spatially incoherent light with a wavelength of 555 nm, corresponding to the highest sensitivity of the human eye in photopic vision [15].

In fact, two conditions were considered: first, the inlays were centered on the visual axis (line of sight) [16] at the inlay

**TABLE 1.** Liou-Brennan model eye Zemax data sheet (*r* and *z* are radial and axial coordinates in the crystalline lens).

Surface	Radius (mm)	Asphericity	Thickness (mm)	Refractive index
Anterior Cornea	7.77	-0.18	0.2	1.376
Anterior CI	7.77	-0.18	0.005	1.376
Posterior CI	7.77	-0.18	0.295	1.376
Posterior Cornea	6.40	-0.60	3.16	1.336
Iris	-	-	0.00	-
Anterior Lens	12.4	-0.94	1.59	1.368 + 0.049057 <i>z</i> - 0.015427 <i>z</i> <sup>2</sup> - 0.001978 <i>r</i> <sup>2</sup>
Lens	Infinity	-	2.43	1.407 - 0.006605 <i>z</i> <sup>2</sup> - 0.001978 <i>r</i> <sup>2</sup>
Posterior Lens	-8.10	0.96	16.26	1.336

plane, and, second, the inlays were decentered of 0.8 mm towards the temporal direction.

The MTF feature of the Zemax OpticStudio was employed to calculate the MTF at the retina for different object vergences. Due to the asymmetry of the model eye, the MTFs in tangential and sagittal directions were different; thus, to obtain a simple measure for the image quality, the arithmetic mean between the tangential and sagittal MTFs was considered. The position of the retina remained the same for all MTF calculations.

**C. EXPERIMENTAL PROCEDURE**

The optical performance of the DCI was experimentally tested in vitro with a custom made image forming system using an ISO eye model [17]. To this end, the inlays, were printed on graphic films (standard polyester films) using a photoplotter with 5080 lpi resolution. In the optical setup, whose description and performance have been described in detail elsewhere [18], the illumination system consisted of a white LED with a band-pass filter (wavelength 560 ± 10 nm) placed behind it to obtain monochromatic images. The test object (1951 USAF resolution test chart) was located in front of an achromatic lens of focal length 160 mm, acting as Badal lens to simulate distance and near vergences. The artificial presbyopic eye was constructed with an achromatic doublet acting as artificial cornea and a wet cell in which a monofocal 10 D intraocular lens (AIALA model F551250; AJL Ophthalmic SA; Álava, Spain) [19], was located. Two different lens holders with diameters 3.0 mm and 4.5 mm were employed as artificial pupils. In the experiment, the printed inlays were located just in front of the cornea lens. An 8-bit CMOS camera (EO-5012C; Edmund Optics, Illinois, USA); attached to an X5 microscope (focused on the far focal plane

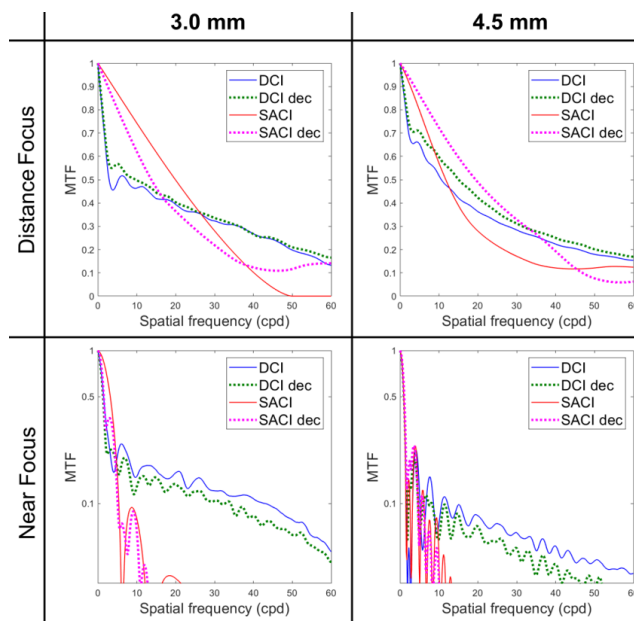


**FIGURE 2.** MTFs for distance and near objects. DCI and SACI curves correspond to the inlays centered on the visual axis. “DCI dec” and “SACI dec” correspond to the inlays decentered 0.8 mm towards the temporal direction.

of the intraocular lens) was used to capture the image of object for two different vergences.

**III. RESULTS**

The results of the MTFs computed for the DCI and SACI inlays are shown in Figure 2. The MTFs for distance focus show that in the range of spatial frequencies from 30 cpd to 60 cpd, which correspond to high rates of visual acuity, the MTF values for the DCI are higher than the SACI for both, centered and decentered conditions. On the other hand, for the near focus, the MTF for the SACI drops to zero. In this case, the MTFs was represented in logarithmic scale from 0.03 to 1 to enhance differences between centered and decentered conditions for the DCI. At this point it is important to note that the harmful diffraction effects produced by the microholes in the SACI were not taken into account. In fact, diffracted light by the pores (5% of the total) would worsen even more the results for the SACI MTFs. [20]. As can be seen, the DCI is more robust against decentrations than SACI. Note that for the distance focus the curve for the SACI drops with the decentration for 3 mm pupil but grows for 4.5 mm pupil. This effect is due to the light that reach the retina coming from the outer part of the annulus. However, in this case the depth of focus is highly reduced [21]. This result can be better appreciated in the AMTF shown in Fig. 3.

The AMTF was computed for different object vergences between +0.5 to -3.5 D (in 0.1D steps), and for spatial frequencies in the range: 9.5 cpd to 59.9 cpd. These frequencies correspond, approximately, to visual acuities between 0.5 logMAR and -0.2 logMAR (assuming that a logMAR of 0 is equivalent to a retinal spatial frequency of 30 cpd

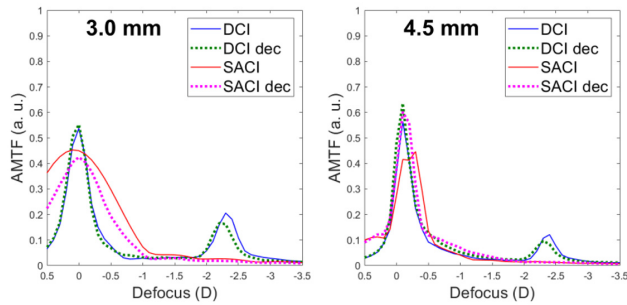


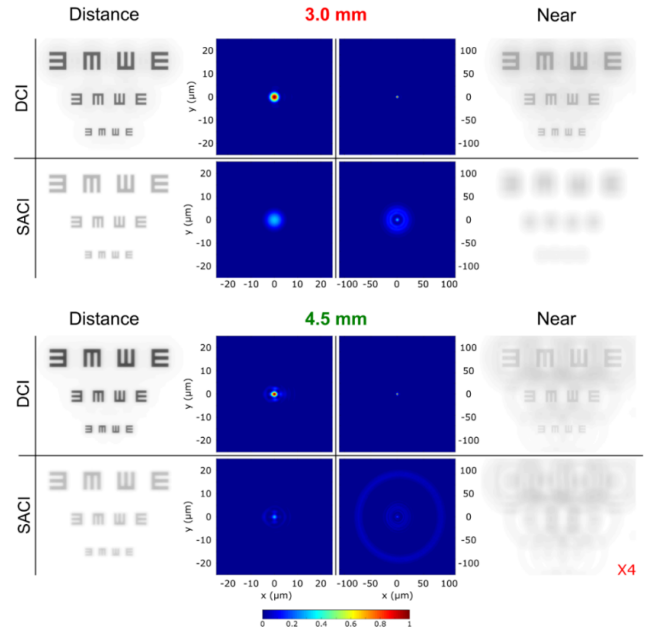
**FIGURE 3.** Through the focus AMTFs. DCI and SACI curves correspond to the inlay centered on the visual axis. “DCI dec” and “SACI dec” correspond to the inlays decentered 0.8 mm towards the temporal direction.

and that scale invariance holds). Note that, as expected [14], the depth of focus of the SACI is very sensitive to both, decentration and pupil diameter. On the contrary, the DCI globally maintains the typical bifocal shape with a little drop at the near focus for 4.5 mm pupil. However, as we will see next, this effect is partially compensated by the increase in the light throughput with this pupil diameter.

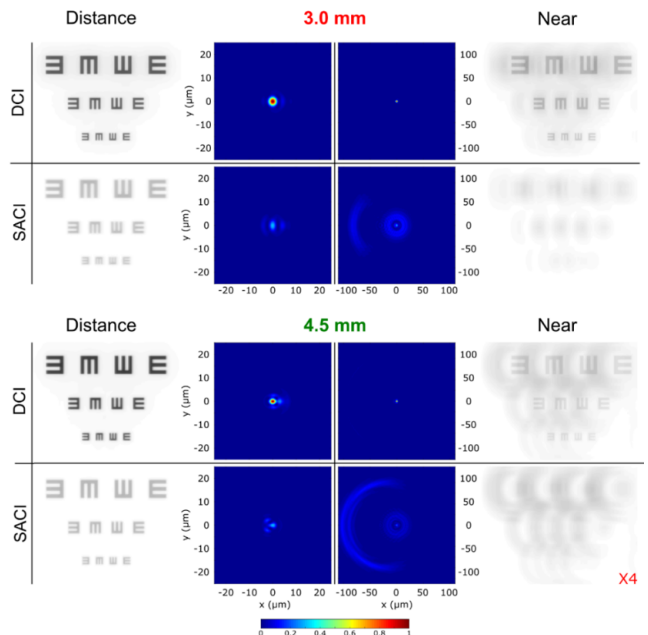
Another useful metric we employed for the comparison of both inlays was the PSF. Moreover, from the PSF provided by ZEMAX, we obtained simulated images of a high contrast visual acuity test chart, by means of the numerical convolution, using a custom Matlab code (Mathworks, Inc. R2018b). Figures 4 and 5 show the PFSs provided by the model eye virtually implanted with both inlays for point objects at far and near distances with two pupil diameters. In these figures, the corresponding simulated images of a high contrast tumbling E chart, with letter sizes corresponding to 0.4 logMAR, 0.2 logMAR and 0 logMAR visual acuities are shown next to the corresponding PSF. The simulated images were obtained as the convolution of the PSF (normalized to the maximum value for each pupil diameter) with the optotype. To obtain the images, after the normalization we imposed the condition of image energy conservation by setting to 1 the sum value of each PSF frame. Then each PSF was weighted by its theoretical relative intensity [9]. In this way, the relative intensity of the images can be directly compared.

Figure 4 shows the results for both inlays centered. As can be seen, the PSF for the DCI is better than the PSF for the SACI in all situations. Note also the different contrast in the images of optotypes, which is a consequence of the relative light throughput of the inlays. With a 3 mm pupil diameter the SACI acts as a circular aperture, but as the pupil diameter increases, additional light enters through the iris aperture producing the halo that is clearly appreciated in the PSFs. Note that in the plots of the PSF at near the scale was extended to 200 microns to show the extension of the halos. In the image of the SACI at near the intensity was multiplied by a factor of 4, because otherwise this (defocused) image would not be noticeable.

It can be verified that for near objects, the eye with the SACI does not resolves the letters of 0.4 logMAR. For 3.0 mm



**FIGURE 4.** PSFs at the far and near foci provided by the DCI and SACI inlays. The corresponding simulated images are shown side by side. For SACI at near the image intensity was enhanced 4 times.



**FIGURE 5.** Idem Fig. 4, but with the inlays decentered 0.8 mm in the temporal direction.

pupil there is a kind of contrast inversion in the image that could help the patient to identify the letters, but for a large pupil the visual acuity decreases, and this would no longer possible.

We want to emphasize that these results for the SACI coincide with those obtained by Schwarz et al. [22] in real eyes with the same optotype, but using a visual simulator based on adaptive optics.

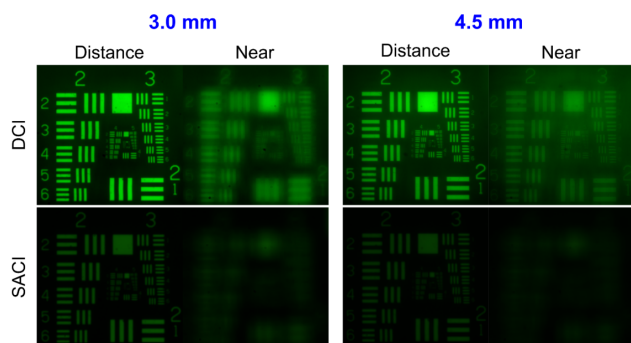


**FIGURE 6.** Experimental images obtained for an artificial presbyopic model eye (ISO 11979-9 Standard) with the DCI and SACI located in just front of the artificial cornea.

Figure 5 is equivalent to Figure 4 but with the inlays decentered 0.8 mm in the temporal direction. By comparing Fig. 4 and Fig. 5, it is clear that the tolerance of the DCI to decentration is much higher than the SACI, because the closer resemblance of the corresponding PSFs at near and distance, for both pupil diameters.

Finally, the images obtained experimentally with the physical inlays in front of model eye cornea are shown in Fig. 6. These images, achieved for the same pupil diameters used in the numerical simulations, demonstrate the light throughput difference between the DCI and the conventional SACI predicted in Fig. 4.

#### IV. DISCUSSION AND CONCLUSION

In this work we have provided evidence of the good performance of the DCI as image forming device in comparison with the commercially available pin-hole based corneal inlay. Both devices were virtually implanted in the Liou–Brennan model eye considering that, in addition to be one of the most physiologically realistic models, its optical parameters are based on measurements of early presbyopes, which are likely the best candidates for corneal inlay surgery. In fact, a similar model eye has been already applied for investigating the effect of the SACI on the peripheral visual field [21]. Additionally, we reported experimental results, obtained in vitro according to the ISO 11979-9 Standard, which also gave a favorable verification for the performance of the DCI in image formation. Specifically, we demonstrated that, compared with the SACI our proposal provides images with high intensity levels. This is important because, current inlays needs to be implanted monocularly in the non-dominant eye, with the risk of significant decline in the patient’s binocular visual performance, compromising stereoacuity [8], and also binocular visual acuity because binocular summation is less effective as the interocular differences in retinal image increase. In fact, Taberero and coworkers [23] found that, the binocular far-distance visual acuity achieved with one eye implanted with SACI comply binocular summation; but, in contrast, the visual acuity for near distance seems to match to the near distance acuity of the eye with SACI. Therefore, according to our results, can assume that even adopting the

same criterion of monocular implantation, the binocular performance of the DCI at near could be better than the SACI, but this is an assumption that should be confirmed in future studies.

On the other hand, considering that the clinical outcomes demonstrated that SACI is very sensitive to centration (even requiring recentration in some cases) [14], another relevant result of this work is that in a realistic model eye, the DCI is more robust against decentration than SACI, as can be seen in Fig. 2 and 3. Moreover, the AMTFs represented in Fig. 3 reveal that the DCI is also less pupil dependent than the SACI. The drop of the depth of focus obtained for the SACI for 4.5 mm pupil, in comparison with the result for 3.0 mm pupil diameter, evident in this figure, can be attributed to the light that passes through the outer part of the inlay, which counteracts the pinhole effect. This effect was not previously found in other studies of the SACI in which the external diameter of the inlay was ignored. In spite of this, the better results obtained for the inlays centered on the visual axis agree with those reported Taberero and Artal [14].

A limitation of this work is that the eye model, despite of being anatomically accurate, it is still a model, that obviously does not reproduce the effect of image processing by the brain. Therefore, as was done for the SACI in the recent years, more theoretical, and above all, clinical work is needed to assess the visual performance in real human eyes. The use of visual simulators could be the first step in this process. In addition, since the intensity ratio of the far and near focal spots can be controlled by adjusting the proportion of the area of the DCI central hole and the surrounding structure, visual simulators could confirm whether this unique feature would allow the construction of customizable corneal implants. Another significant consequence of the improved light throughput of the DCI could be its bilateral implantation. Summarizing: Bifocality, high transmission efficiency, and robustness against decentration are benefits of the DCI not previously achieved simultaneously by any other corneal inlay.

#### REFERENCES

- [1] W. N. Charman, “Developments in the correction of presbyopia II: Surgical approaches,” *Ophthalmic Physiol. Opt.*, vol. 34, no. 4, pp. 397–426, Jul. 2014.
- [2] E. M. Arlt, E. M. Krall, S. Moussa, G. Grabner, and A. K. Dextl, “Implantable inlay devices for presbyopia: The evidence to date,” *Clin. Ophthalmol.*, vol. 9, pp. 129–137, Jan. 2015.
- [3] R. L. Lindstrom, S. M. MacRae, J. S. Pepose, and P. C. Hoopes, “Corneal inlays for presbyopia correction,” *Current Opinion Ophthalmol.*, vol. 24, no. 4, pp. 281–287, Jul. 2013.
- [4] S. Vilupuru, L. Lin, and J. S. Pepose, “Comparison of contrast sensitivity and through focus in small-aperture inlay, accommodating intraocular lens, or multifocal intraocular lens subjects,” *Amer. J. Ophthalmol.*, vol. 160, no. 1, pp. 150–162, Jul. 2015.
- [5] J. A. Vukich, D. S. Durrie, J. S. Pepose, V. Thompson, C. van de Pol, and L. Lin, “Evaluation of the small-aperture intracorneal inlay: Three-year results from the cohort of the U.S. Food and drug administration clinical trial,” *J. Cataract Refractive Surg.*, vol. 44, no. 5, pp. 541–556, May 2018.
- [6] J. Gilchrist and S. Pardhan, “Binocular contrast detection with unequal monocular illuminance,” *Ophthalmic Physiol. Opt.*, vol. 7, no. 4, pp. 373–377, Oct. 1987.

- [7] S. Plainis, D. Petratou, T. Giannakopoulou, H. Radhakrishnan, I. G. Pallikaris, and W. N. Charman, "Small-aperture monovision and the pulfrich experience: Absence of neural adaptation effects," *PLoS One*, vol. 8, no. 10, Oct. 2013, Art. no. e75987.
- [8] J. J. Castro, C. Ortiz, J. R. Jiménez, S. Ortiz-Peregrina, and M. Casares-López, "Stereopsis simulating small-aperture corneal inlay and monovision conditions," *J. Refract. Surg.*, vol. 34, no. 7, pp. 482–488, Jul. 2018.
- [9] W. D. Furlan, S. García-Delpech, P. Udaondo, L. Remón, V. Ferrando, and J. A. Monsoriu, "Diffractive corneal inlay for presbyopia," *J. Biophotonics*, vol. 10, no. 9, pp. 1110–1114, Sep. 2017.
- [10] L. Kipp, M. Skibowski, R. L. Johnson, R. Berndt, R. Adelung, S. Harm, and R. Seemann, "Sharper images by focusing soft X-rays with photon sieves," *Nature*, vol. 414, pp. 184–188, Nov. 2001.
- [11] F. Giménez, J. A. Monsoriu, W. D. Furlan, and A. Pons, "Fractal photon sieve," *Opt. Express*, vol. 14, no. 25, pp. 11958–11963, Jan. 2006.
- [12] H.-L. Liou and N. A. Brennan, "Anatomically accurate, finite model eye for optical modeling," *J. Opt. Soc. Amer. A, Opt. Image Sci.*, vol. 14, no. 8, pp. 1684–1695, Aug. 1997.
- [13] R. C. Bakaraju, K. Ehrmann, E. Papas, and A. Ho, "Finite schematic eye models and their accuracy to *in-vivo* data," *Vis. Res.*, vol. 48, no. 16, pp. 1681–1694, Jul. 2008.
- [14] J. Taberero and P. Artal, "Optical modeling of a corneal inlay in real eyes to increase depth of focus: Optimum centration and residual defocus," *J. Cataract Refractive Surg.*, vol. 38, no. 2, pp. 270–277, Feb. 2012.
- [15] H. Gross, F. Blechinger, and B. Ahtner, *Handbook of Optical Systems* (Survey of Optical Instruments), vol. 4. Hoboken, NJ, USA: Wiley, 2008.
- [16] J. T. Schwiegerling, "Eye axes and their relevance to alignment of corneal refractive procedures," *J. Refractive Surg.*, vol. 29, no. 8, pp. 515–516, Aug. 2013.
- [17] *Ophthalmic Implants—Intraocular Lenses—Part 2: Optical Properties and Test Methods*, Standard ISO 11979-2:2014, 2014.
- [18] A. Calatayud, L. Remón, J. Martos, W. D. Furlan, and J. A. Monsoriu, "Imaging quality of multifocal intraocular lenses: Automated assessment setup," *Ophthalmic Physiol. Opt.*, vol. 33, no. 4, pp. 420–426, Jul. 2013.
- [19] W. D. Furlan, L. Remón, C. Llorens, M. Rodríguez-Vallejo, and J. A. Monsoriu, "Comparison of two different devices to assess intraocular lenses," *Optik*, vol. 127, no. 20, pp. 10108–10114, Oct. 2016.
- [20] W. N. Charman, Y. Liu, and D. A. Atchison, "Small-aperture optics for the presbyope: Do comparable designs of corneal inlays and intraocular lenses provide similar transmittances to the retina?" *J. Opt. Soc. Amer. A, Opt. Image Sci.*, vol. 36, no. 4, pp. B7–B14, Apr. 2019.
- [21] D. A. Atchison, S. Blazaki, M. Suheimat, S. Plainis, and W. N. Charman, "Do small-aperture presbyopic corrections influence the visual field?" *Ophthalm. Physiol. Opt.*, vol. 36, no. 1, pp. 51–59, Jan. 2016.
- [22] C. Schwarz, S. Manzanera, P. M. Prieto, E. J. Fernández, and P. Artal, "Comparison of binocular through-focus visual acuity with monovision and a small aperture inlay," *Biomed. Opt. Express*, vol. 5, no. 10, pp. 3355–3366, Oct. 2014.
- [23] J. Taberero, C. Schwarz, E. J. Fernández, and P. Artal, "Binocular visual simulation of a corneal inlay to increase depth of focus," *Investigative Ophthalmology Vis. Sci.*, vol. 52, no. 8, pp. 5273–5277, Jul. 2011.



**DIEGO MONTAGUD-MARTÍNEZ** was born in Valencia, Spain, in 1984. He received the bachelor's degree in chemistry and the master's degree in optics and optometry from the Universitat de València, and the master's degree in vision sciences from the Universitat de València. He is currently pursuing the Ph.D. degree with the Diffractive Optics Group, Universitat Politècnica de València. He was with the Laboratorio de Óptica de la Universidad de Murcia Laboratorio de Óptica de la Universidad de Murcia. He earned the extraordinary award of optics and optometry.



**VICENTE FERRANDO** was born in Valencia, Spain, in 1986. He received the B.S. degree in physics and the M.S. degree in advanced physics (photonics) from the Universitat de València, Valencia, Spain, in 2010 and 2012, respectively, and the Ph.D. degree from the Universitat Politècnica de València, Valencia, in 2017. Since 2011, he has been a Researcher with the Diffraction Optics Group, Universitat de València and the Universitat Politècnica de València. His current research interest includes optical properties of aperiodic diffractive lenses and their applications.



**FEDERICO MACHADO** was born in San Salvador, El Salvador, in 1970. He received the B.S. degree in electrical engineering from the Universitat Politècnica de València, San Salvador, El Salvador, the M.S. degree in the management of renewable resources from the Universidad Don Bosco, Antiguo Cuscatlan, El Salvador, in 1993 and 2013, respectively, and the Ph.D. degree with the Universitat Politècnica de València, Valencia, Spain. He was with the Universidad Don Bosco for 15 years in different positions, teaching subjects related to electrical, electronics, and renewable resources. His research interests include energy efficiency and designing electronic systems to support educational systems.



**JUAN A. MONSORIU** was born in Valencia, Spain, in 1975. He received the B.S. degree in physics, the M.S. degree in optics, and the Ph.D. degree in physics from the Universitat de València, Valencia, in 1998, 2000, and 2003, respectively. In 2000, he joined the Universitat Politècnica de València (UPV), Valencia, where he is currently a Full Professor of Applied Physics. His research has been performed at the UV, the UPV, the Universidad de Málaga, Spain, the University of Bath, U.K., and the Universidad de Buenos Aires, Buenos Aires, Argentina. His main research interests include numerical simulations for the design of microstructured optoelectronic systems and aperiodic optical devices.



**WALTER D. FURLAN** received the M.S. and Ph.D. degrees in physics from the University of La Plata, La Plata, Argentina, in 1984 and 1988, respectively. He was with the Centro de Investigaciones Ópticas, Argentina, until 1990. At the end of 1990, he joined the Department of Optics, Universitat de València, Valencia, Spain, where he is currently a Professor of optics. He is currently a Full Professor and the Co-Director of the Diffractive Optics Group. His research has been developed in the field of optics in two well differentiated areas. In these topics, he has authored or coauthored more than 25 articles in refereed journals and chapters in *Phase-Space Optics: Fundamentals and Applications* (McGraw-Hill, 2009). On the other hand, mainly in the last ten years, he has focused on the study of the properties of nonconventional diffractive optical elements. On the one hand, he has investigated on the theory and applications of phase-space representations (Wigner distribution function and ambiguity function). He has coauthored more than 30 articles. He held three patents related to his research topics. He is a member of the European Optical Society.

...